TILTING PAD BEARING DESIGN

by
John C. Nicholas
Chief Engineer
Rotating Machinery Technology, Incorporated
Wellsville, New York

John Nicholas received his B.S.A.E. degree from the University of Pittsburgh (1968) and his Ph.D. degree from the University of Virginia (1977) in rotor and bearing dynamics. While at Virginia, he authored the tilting pad and pressure dam bearing computer programs that are used by many rotating equipment vendors, users, and consultants.

Dr. Nicholas has worked in the turbomachinery industry for the last 17 years in the rotor and bearing dynamics areas, including five years at Ingersoll-Rand and five years as the Supervisor of the Rotordynamics Group at Dresser-Rand.

Currently, Dr. Nicholas is part owner and Chief Engineer for Rotating Machinery Technology, Incorporated, a company that manufactures high performance tilting pad journal and thrust bearings, sleeve bearings, and seals for the rotating equipment industry for the last six years.

Dr. Nicholas, a member of ASME, STLE, and the Vibration Institute, has authored 27 technical papers concerning tilt pad bearing dynamics, pressure dam bearings, rotordynamics and support stiffness effects on critical speeds.

ABSTRACT

The basics of tilting pad bearing design are discussed to include limits of operation for load, speed, and metal temperature. Optimum temperature sensor locations are recommended for self aligning and nonaligning tilting pads. Tilting pad bearing geometric properties and their influence on bearing and rotordynamics are addressed including the advantages and disadvantages of zero preloaded pads. Also, the advantages of increasing the pad axial length are shown.

Example calculations are presented for the tilting pad pivot film thickness which is necessary to determine if the top pads are loaded or unloaded. Tilting pad static shaft sink and clearance measurement techniques are addressed. The equations to calculate normal force and break away torque are derived including an example calculation comparing a tilting pad bearing to a two axial groove bearing. Tilting pad bearing oil flow and temperature rise are included along with a discussion of reduced temperature tilting pad designs.

INTRODUCTION

As the speeds of turbomachinery are increased in order to improve aerodynamic performance, bearing designs are stretched to their limit and, in some cases, beyond. It is becoming increasingly important for the bearing designer to use every design tool possible to ensure that bearings will operate satisfactory for these high performance applications.

To this end, many of the design considerations for high performance bearings are discussed in an effort to establish general design guidelines for tilt pad bearing design. It must be understood, however, that there are always exceptions to any rule. Therefore, the conclusions and recommendations are meant to be used as a starting point or guide for the bearing designer when designing high performance tilting pad bearings.

JOURNAL BEARING LIMITS OF OPERATION

A two axial groove sleeve bearing is illustrated in Figure 1 supporting a vertically downward load with a displacement that is not directly downward, but at some attitude angle, with rotation from bottom dead center. This property of sleeve bearings is responsible for producing destabilizing cross coupling forces that cause oil whirl (exactly 50 percent of synchronous speed vibration) and/or shaft whip (reexcitation of the rotor's first critical speed at a frequency that is less than 50 percent of synchronous speed).

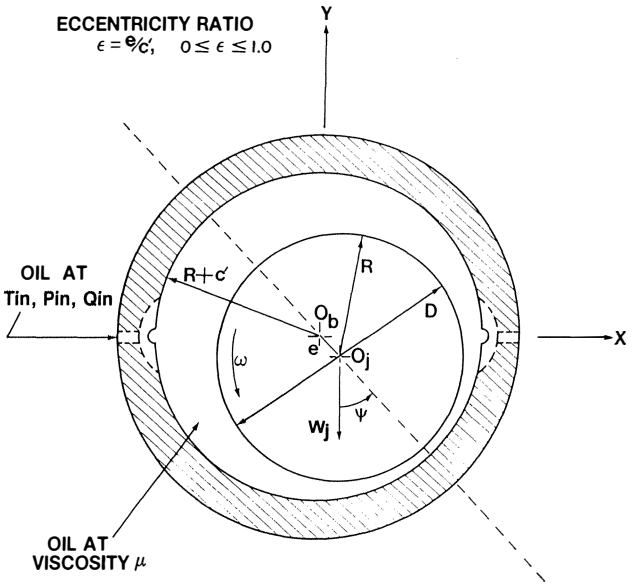

Figure 1. Two Axial Groove Bearing.

This phenomena is most prevalent at high speeds and/or light loads. For this reason, in addition to a high load design limit, a low load limit is also placed on sleeve bearings. Define the bearing unit load as

$$L_u = \frac{W_j}{L \cdot D} \tag{1}$$

For sleeve bearings, suggested load design limits are

$$L_u \leq 200 \text{ psi} \tag{2}$$

$$L_u \geq 100 \text{ psi} \tag{3}$$

Ideally, a sleeve bearing should be designed between these limits. However, bearings with higher unit loads can operate without problems as long as care is taken to properly cool the bearing. That is, unit loads above the design limit may require higher oil flows and/or a reduced temperature design similar to those discussed in a later section.

The lower load limit may be relaxed somewhat if a stabilized sleeve bearing design such as a pressure dam or multilobe bearing is used.

A journal surface velocity limit should also be noted. Define the surface velocity as

$$U_s = \left(\frac{\pi}{30}\right) \cdot \left(\frac{N \cdot R}{12}\right) \tag{4}$$

The recommended journal surface velocity upper design limit is

$$U_s \leq 300 \text{ f/s} \tag{5}$$

Again, this limit may be exceeded, but care must be taken to properly cool the bearing.

Typical bearing clearances range from 1.5 to 2.0 mils of diametral clearance per inch of journal diameter. The 2.0 mil/in rule is normally used at higher journal speeds (above 12,000 rpm) with even higher values for very high speeds. Bearings run cooler as the clearance increases. Unfortunately, the bearings effective damping may decrease with increasing clearance causing increased shaft vibration levels. This is particularly true for rotors that operate below their first bending critical speed such as gear driven double overhung twin pinion compressors used in air separation service.

A sleeve bearings hydrodynamic circumferential pressure profile is shown in Figure 2 for a vertically downward journal load. Note that the maximum hydrodynamic pressure is not located at bottom dead center (i.e., the journal load direction), but is clocked at some angle *with* rotation from vertically downward.

Furthermore, the maximum film temperature is located very near the maximum pressure. Thus, embedded temperature sensors should be placed at some angle with rotation from bottom dead center for horizontal rotors with vertically downward journal loads. If the exact location of the maximum pressure is unknown, it is preferable to sense the film temperature downstream of the maximum temperature location. The 45 degrees with rotation from bottom dead center location is a good rule-of-thumb, if the location of the maximum pressure is unknown.

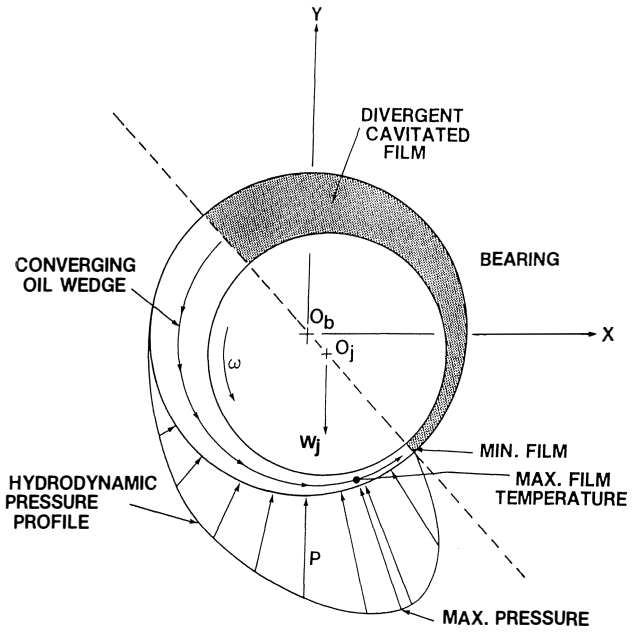

Figure 2. Sleeve Bearing Hydrodynamic Pressure Profile.

The maximum embedded temperature sensor limits are summarized below:

$$\begin{aligned} T_{max} &\leq 185 \text{ °F design (analytical prediction)} \\ T_{max} &\leq 200 \text{ °F test acceptance} \\ T_{max} &\geq 230 \text{ °F alarm} \\ T_{max} &\geq 250 \text{ °F trip} \end{aligned} \tag{6}$$

The bearing babbitt actually melts at around 455°F. However, it does get soft at around 250 to 275°F. At these temperatures, the babbitt will start to wipe or smear. This wiping is more severe for high bearing unit loads. Thus, the maximum unit load limit and maximum bearing or babbitt temperature limit are coupled.

Note that the maximum oil temperature will be somewhat higher than the maximum embedded temperature. A rough estimate is to add about 20°F to the embedded temperature to obtain the oil film temperature.

For lightly loaded bearings, a high temperature bearing failure will usually cause the oil to break down and leave a dark coating on the babbitt surface. The oil loses its viscosity and the bearing clearance is reduced. For heavily loaded bearings, wiping usually occurs before oil breakdown.

TILTING PAD JOURNAL BEARING LIMITS OF OPERATION AND TEMPERATURE SENSOR LOCATION

All of the above limits apply to tilting pad bearings with the exceptions noted in this section. A tilting pad bearing with between pivot loading is illustrated in Figure 3. Note that the journal sinks straight down in the bearing, thereby producing zero destabilizing cross coupling forces. Thus, the lower unit load design limit imposed on sleeve bearings for stability reasons can be removed for tilting pad bearings. The upper unit load limit remains at

$$L_u \leq 200 \text{ psi} \tag{7}$$

The angle of pad tilt and the maximum film pressure and temperature are shown in Figure 4. The pads leading edge tilts open to provide a converging wedge to produce hydrodynamic load. The resultant load vector passes through the pad pivot.

As before, the maximum pressure is located not at the pad pivot location, but at some angle with rotation from the pivot. Thus, temperature sensors should be placed downstream from the pivot. A good rule-of-thumb is to locate the sensor at the 75 percent position as in thrust bearings. That is, at 75 percent of the total pad arc length from the leading edge (Figure 5).

Furthermore, the axial location of the maximum pressure and temperature is at the pad axial centerline. This should be the location of the sensor (Figure 6). However, this is only true for pads that have self axial aligning capabilities, as shown in Figure 6. For nonaligning pads, shaft-to-bearing pad misalignment will cause the maximum pressure and temperature to move off centerline toward the side with the smaller film thickness. Thus, for nonaligning pads, two axially side-by-side sensors should be used to ensure detection of the maximum temperature (Figure 7).

Also, these tandem sensors can assist in the detection of pad-to-shaft misalignment. For zero misalignment, both sensors

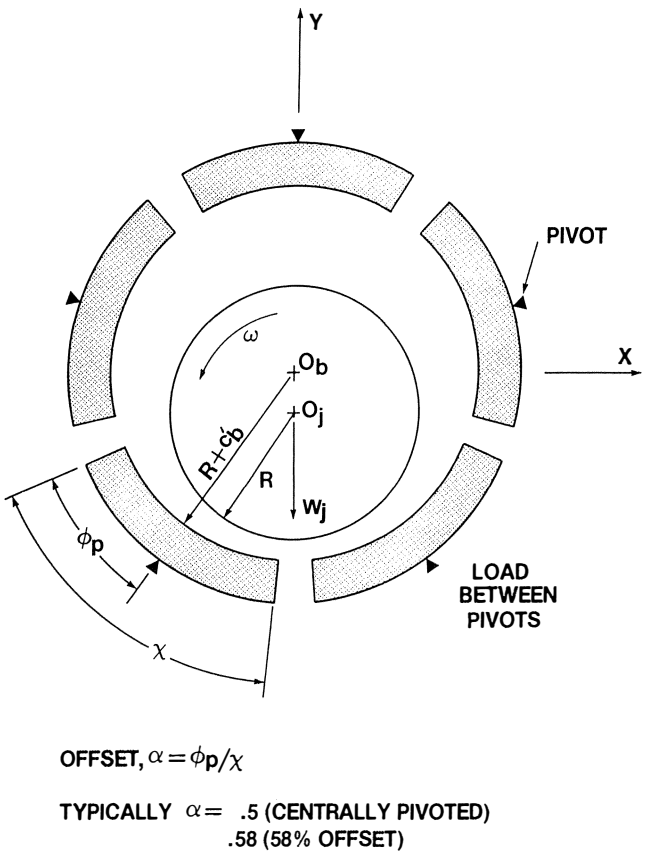

Figure 3. Tilting Pad Bearing—Load Between Pivots.

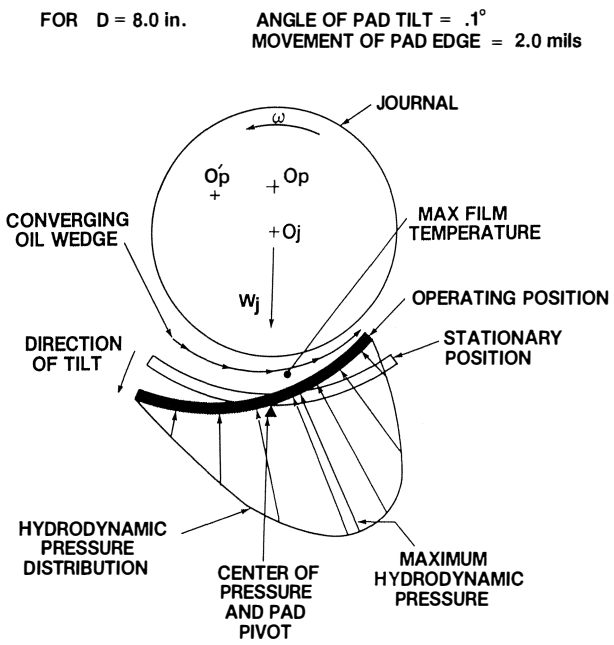

Figure 4. Tilting Pad—Angle of Tilt.

should read the same. Conversely, one sensor will read a higher temperature compared to the other if misalignment exists. The larger the temperature difference, the greater the misalignment.

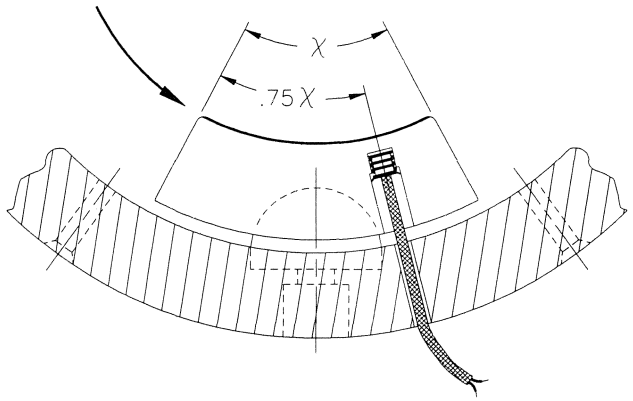

Figure 5. Temperature Sensor Circumferential Location.

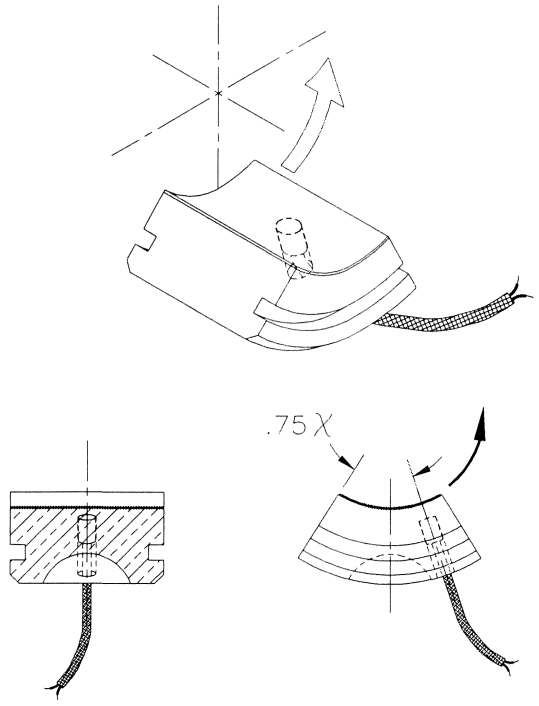

Figure 6. Self Aligning Pad Temperature Sensor Location.

For the load between pivot case, sensors should be mounted in the two bottom loaded pads (Figure 8). While these two sets of sensors should read approximately the same values, the downstream pad usually runs hotter, because it receives hot oil from the upstream loaded pad as illustrated in Figure 8.

A load on pivot tilt pad bearing is presented in Figure 9, where the bottom loaded pad should contain the sensors. In this case, since only one pad is instrumented, a dual element sensor is recommended for redundancy.

The maximum temperature design limits of Equation (6) remain valid for tilting pad bearings.

TILTING PAD BEARING GEOMETRIC PROPERTIES

One advantage of tilting pad bearings is the many design parameters that are available for variation [1, 2 and 3]. The load between pivot configuration is shown in Figure 3 while the load on pivot case may be seen in Figure 10. Load between pads

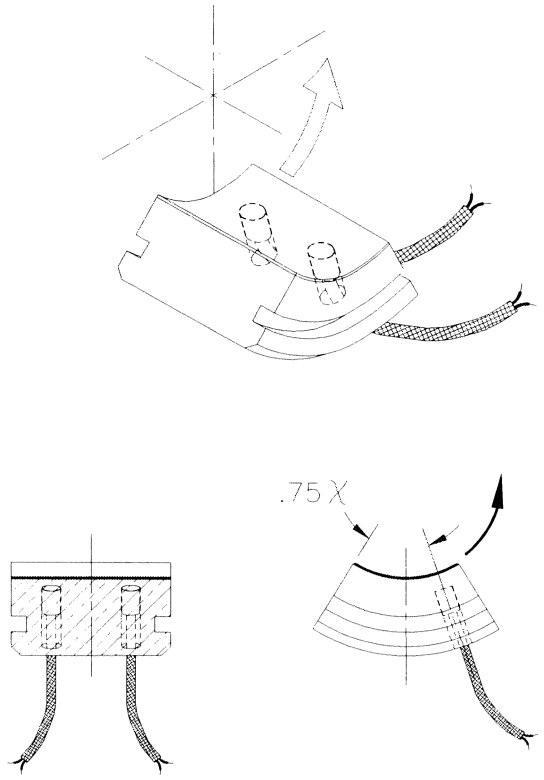

Figure 7. Nonaligning Pad Temperature Sensor Location.

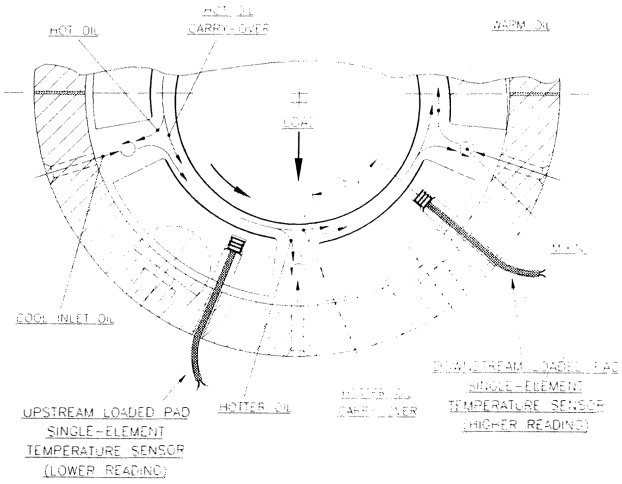

Figure 8. Temperature Sensor Location—Load Between Pads.

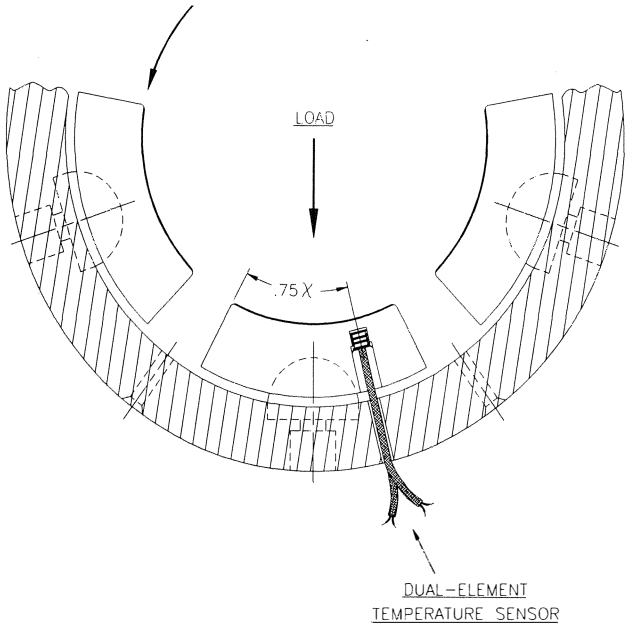

Figure 9. Temperature Sensor Location—Load On Pad.

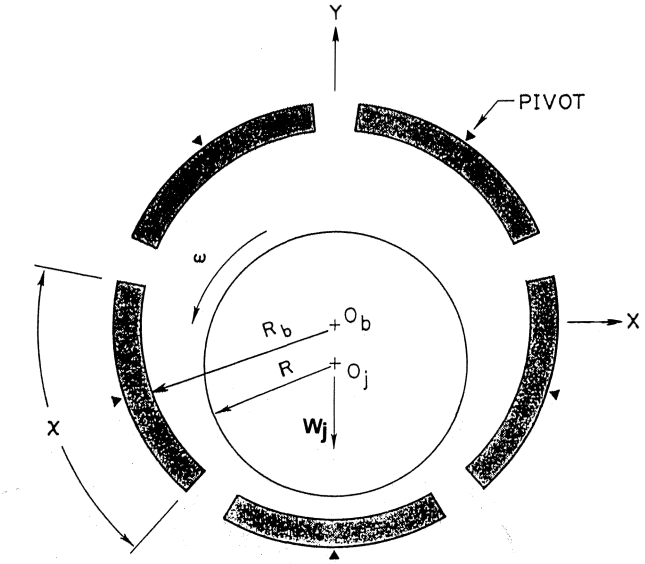

Figure 10. Tilting Pad Bearing—Load On Pivot.

provides more symmetric stiffness and damping coefficients. This is illustrated in Figure 11 [1] where the xx and yy values for K and C approach extreme asymmetry as the Sommerfeld number decreases for the load on pad case. For load between pads (between pivots), the xx and yy values are very close for the entire Sommerfeld number range.

Symmetric support properties provide circular orbits, whereas asymmetric supports cause the elliptical orbit shown in Figure 12. Circular orbits are preferable since, in general, their vibration amplitudes are smaller going through a critical compared to the major axis of an elliptical orbit.

Referring to Figure 3, define the pad pivot offset as

$$\alpha = \frac{\phi_p}{\chi} \tag{8}$$

For centrally pivoted pads, $\alpha = 0.5$ (50 percent offset). Typical offset pivot values range from $\alpha = 0.55$ to $\alpha = 0.6$ (55 to 60 percent offset).

Offset pivots are very popular with thrust bearings, as offsetting the pivot increases the operating film thickness, thereby decreasing the operating temperature (i.e., increases the load capacity). For tilt pad journal bearings, offset pivots also increase load capacity. This is shown at the top of the plot in Figure 13 [1]. For a given Sommerfeld number, S = 1.0 for example, the

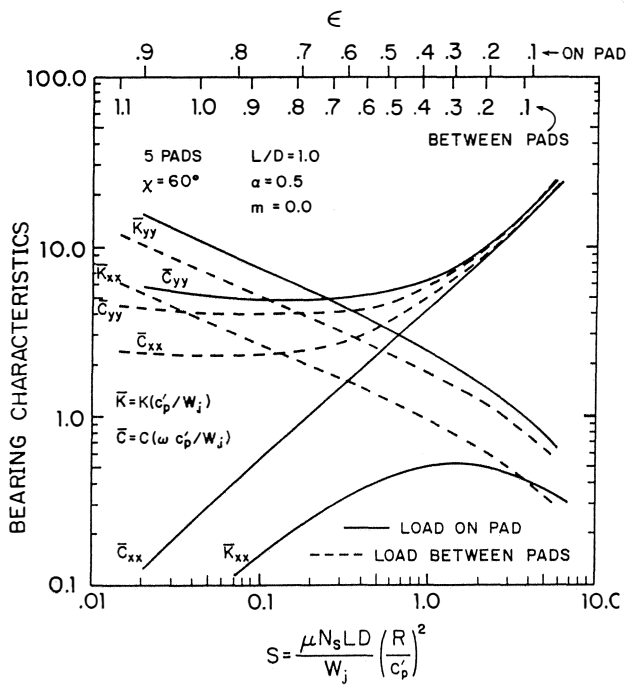

Figure 11. Tilting Pad Bearing—On Pad Vs *Between Pad Loading.*

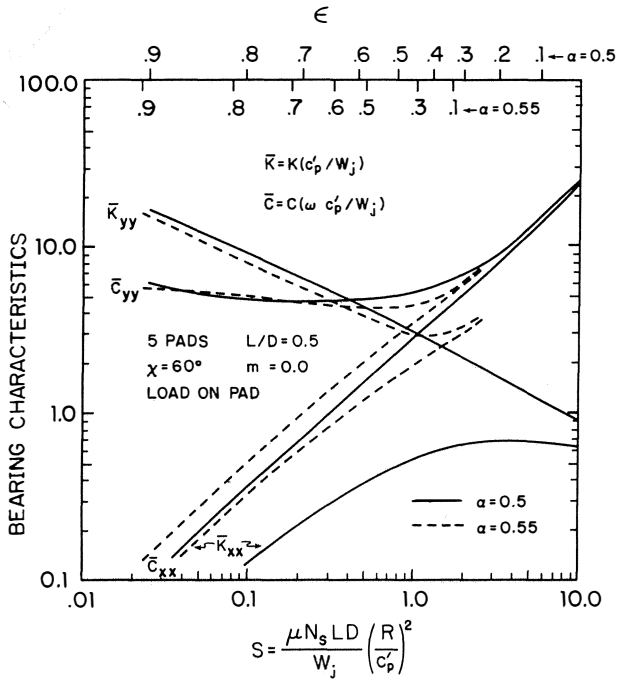

Figure 13. Tilting Pad Bearing—Center Vs *Offset Pivots.*

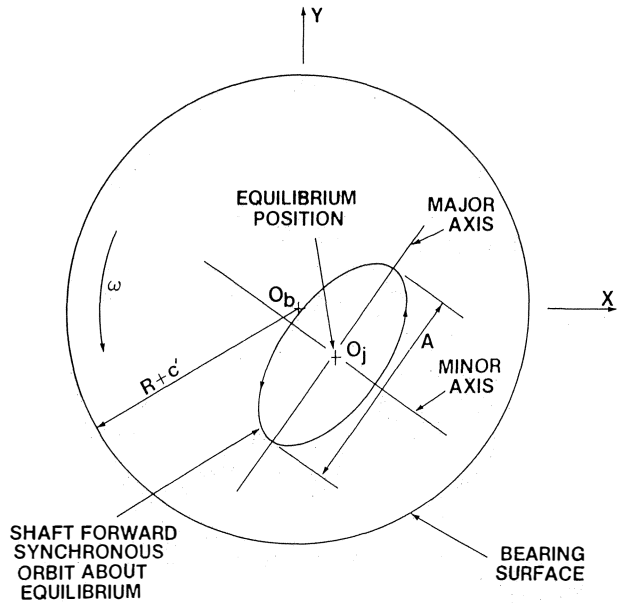

Figure 12. Elliptical Vibration Orbit.

operating eccentricity ratio is 0.45 for centrally pivoted pads compared to 0.3 for $\alpha = 0.55$. Lower values of eccentricity ratio mean higher operating minimum film thicknesses and, thus, higher load capacity. Also, offset pivots increase bearing stiffness, especially K_{xx}, compared to centrally pivoted pads (Figure 13).

TILTING PAD BEARING PRELOAD

Possibly the most important tilting pad bearing parameter available to the bearing designer is tilting pad bearing preload. Referring to Figure 14, tilting pad bearing preload is defined as

$$m = 1 - \left(\frac{C_b}{C_p}\right) \tag{9}$$

The zero preload case is shown in Figure 14, where the pad radius of curvature equals the pivot radius ($R_p = R_b$), and the pad clearance equals the bearing clearance ($c_p = c_b$). When the bearing and journal centers coincide, the journal-to-pad radial clearance at any circumferential location along the pad is constant and equal to c'_b, the bearing radial clearance.

A preloaded pad is illustrated in Figure 15. Now, the pad clearance is greater than the bearing clearance ($c_p > c_b$). Typical

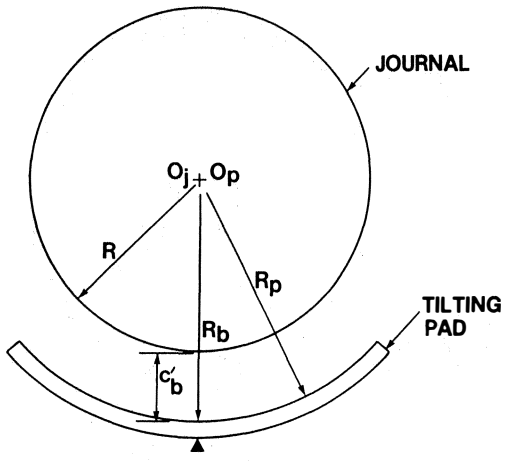

Figure 14. Zero Preloaded Tilting Pad.

preload values range from 0.2 to 0.6 (20 percent to 60 percent). When a pad is preloaded, a converging film section exists and the pad will produce hydrodynamic forces even if the bearing load approaches zero.

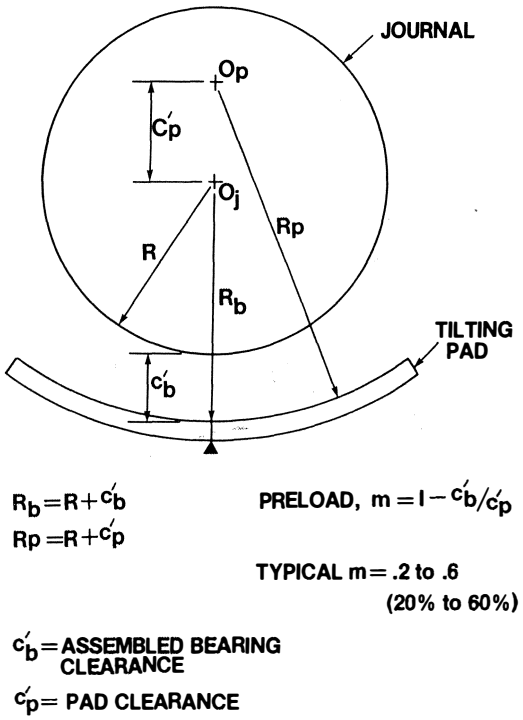

Figure 15. Preloaded Tilting Pad.

ZERO PRELOAD ADVANTAGES AND DISADVANTAGES

The biggest advantage of reducing the tilting pad preload to zero or near zero is illustrated in Figure 16 [3]. For this tilt pad bearing example, as preload decreases, bearing damping increases while bearing stiffness remains approximately constant. Both of these trends help in increasing the bearing effective damping. This trend generally holds for a majority of turbomachinery applications.

Effective damping is a measure of how much bearing damping is effective in shaft vibration suppression. As effective damping increases, shaft vibration decreases. Bearing stiffness has a big influence on the amount of effective damping that a bearing produces. Normally, as bearing damping increases, bearing stiffness increases.

This trend can be seen from Figure 16. As bearing assembled clearance decreases for a constant preload, bearing stiffness and damping both increase. Even though bearing damping increases, the effective damping decreases because the corresponding increase in bearing stiffness makes the bearing damping less effective. The increased bearing stiffness prohibits the shaft from moving in the bearing thereby reducing the effectiveness of the oil film produced damping.

The beneficial effect of decreasing preload for another tilting pad bearing example is illustrated in Figure 17 [4]. In this case, as preload decreases from m = 0.6 to m = 0.0, the bearing damping increases while the bearing stiffness decreases. Again, both of these effects contribute to increasing effective damping.

The influence on rotor stability for the bearings in Figure 17 may be seen in Figure 18 for an eight stage centrifugal compressor [4]. As preload decreases from 0.6 to 0.0, the general trend is to stabilize the compressor (i.e., move the rotor bearing system from well within the unstable regime to well within the stable area of large negative growth factors).

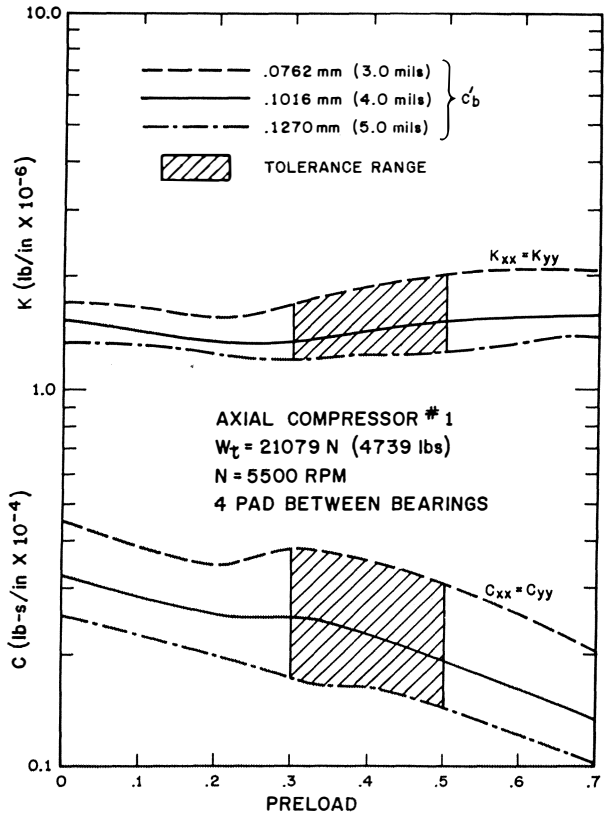

Figure 16. Tilting Pad Bearing Stiffness and Damping vs *Preload and Bearing Clearance.*

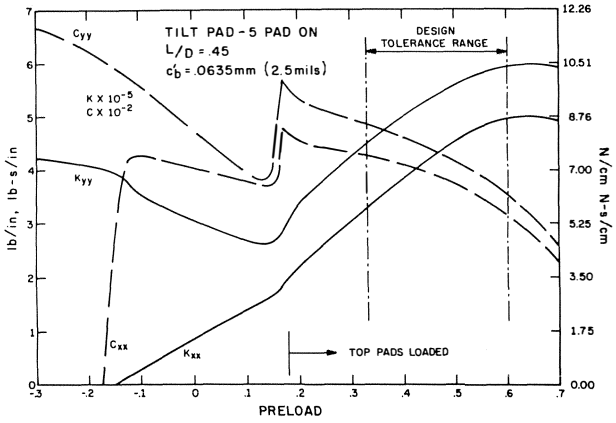

Figure 17. Tilting Pad Bearing—Effect of Negative Preload and Unloaded Top Pads.

Since this is typical of many rotor bearing systems, the temptation to decrease tilt pad preload to near zero to improve machine stability is strong. However, there are several major disadvantages to low preload pads, two of which can be seen in Figures 17 and 18.

First, note the drastic decrease in horizontal stiffness and damping (K_{xx} and C_{xx}) as the pad preload becomes negative in

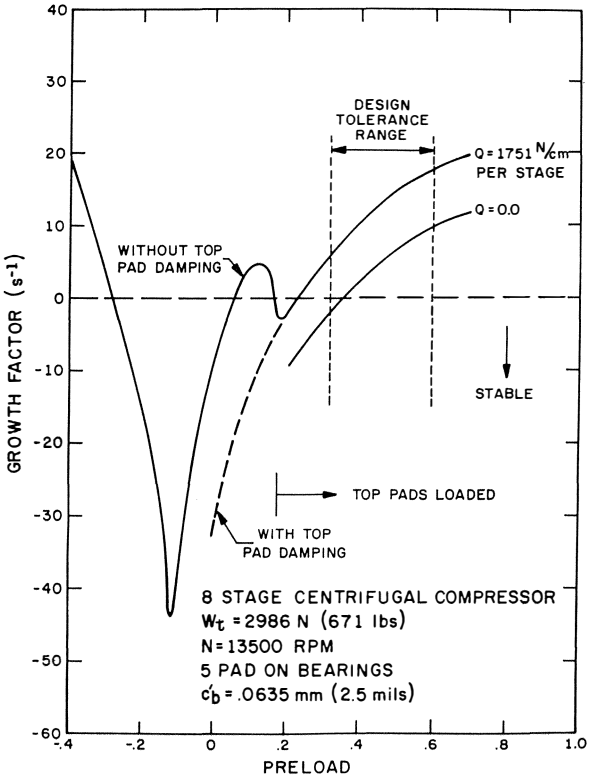

Figure 18. Stability vs Preload—Effect of Top Pad Damping.

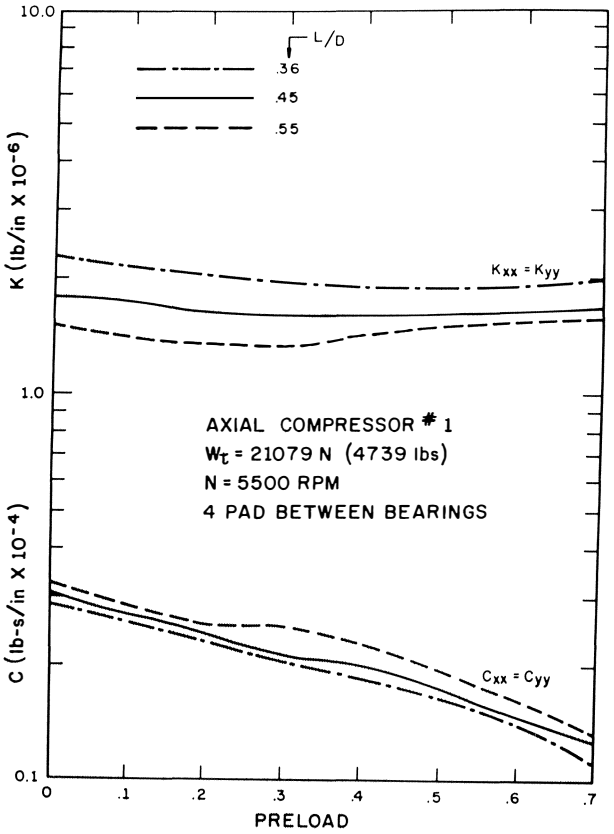

Figure 19. Stiffness and Damping Vs *Preload and Pad L/D Ratio.*

Figure 17. The corresponding effect on stability can be seen in Figure 18 where the system approaches the unstable regime for preload values less than -0.1. The problem is the tolerance range. If zero preload is desired, the tolerance range on the journal diameter, the pad radius of curvature and the assembled bearing clearance can all contribute to producing a negative preload.

The second problem with light preload is the loss of damping when the top pads become unloaded (Figure 17). This condition is addressed in detail in a following section. The rotor bearing system is shown in Figure 18 reverting back into the unstable region after the preload is decreased sufficiently to unload the top pads. Top unloaded pads also flutter, since there does not exist a tilt angle at which the pad can seek equilibrium. Fluttering pads may cause rotor vibration.

PAD L/D RATIO

Another powerful design parameter available to the tilting pad bearing designer is pad length-to-diameter ratio, L/D. An example where increasing the pad L/D ratio increases bearing damping, but decreases bearing stiffness is shown in Figure 19 [3]. Again, both changes contribute to the increase in effective damping.

Of course, it is usually more practical to increase the pad length as opposed to decreasing the journal diameter. For this reason, longer pad lengths have become more popular with the bearing designers. The old standard pad L/D = 0.5 is often replaced by L/D = 0.75 or, in extreme cases, with L/D = 1.0.

The axial length envelop is often restrictive, but if narrow oil end seals are designed correctly, larger pad lengths are often possible. Furthermore, as pad length increases, the pad becomes more susceptible to pad-to-shaft misalignment. Thus, a self aligning pivot should be used for the larger L/D ratios.

PRELOAD AND UNLOADED PADS

In order to determine if a pad is unloaded for a given preload and eccentricity, the bearing oil film thickness at the pad pivot must be calculated. The pivot film thickness, h_p, is illustrated in Figure 20 for a single pad and Figure 21 for an assembled bearing.

$$\bar{h}_p = (1 - m) \cdot (1 + \varepsilon \sin \phi) \tag{10}$$

where

$$\bar{h}_p = \frac{h_p}{c'_p} = \text{pivot film thickness, dim} \tag{11}$$

$$\varepsilon = \frac{e}{c'_b} = \text{bearing eccentricity ratio, dim} \tag{12}$$

Tilting pads become unloaded when there no longer exists a converging film thickness between pad and shaft. This condition exists when the pivot film thickness becomes equal to or greater than the pad radial clearance. Thus, for an unloaded pad,

$$\begin{aligned} h_p &\geq c'_p \\ \bar{h}_p &\geq 1.0 \end{aligned} \tag{13}$$

Setting $\bar{h}_p = 1.0$ and solving for m_b yields

$$m = \frac{\varepsilon \sin \phi}{1 + \varepsilon \sin \phi} \tag{14}$$

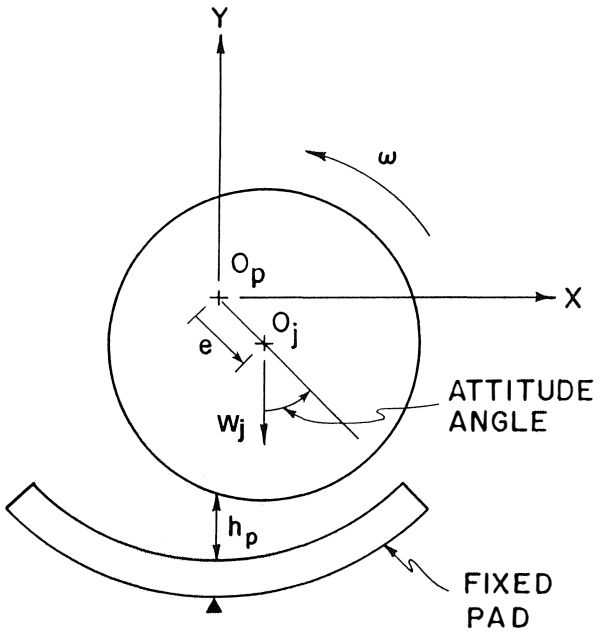

Figure 20. Single Pad Pivot Film Thickness.

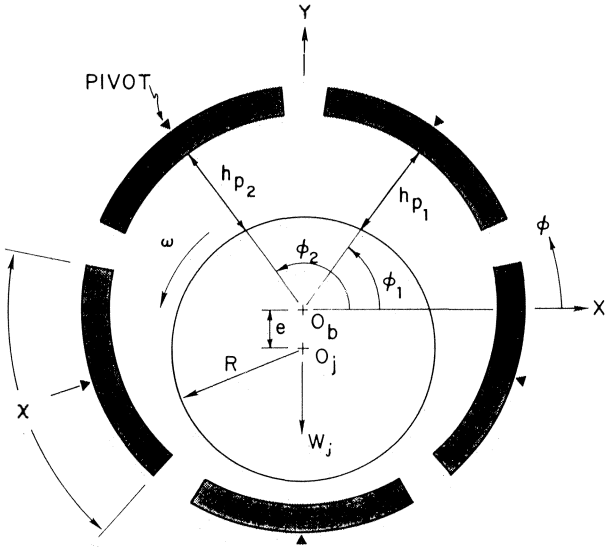

Figure 21. Tilting Pad Bearing Pivot Film Thickness.

The preload is given in Equation 14 *below* which the tilting pad becomes unloaded for a given bearing eccentricity rato, ε.

Also, for $\overline{h_p}$ = 1.0 and for a given preload, the bearing eccentricity ratio, ε, can be calculated *above* which the tilting pad becomes unloaded.

$$\varepsilon = \frac{m}{(1 - m)\sin\phi} \tag{15}$$

Example 1: Calculate the preload at which the top pads of a five pad, load on pivot bearing become unloaded. Assume that the bearing is operating at a moderate eccentricity ratio of ε = 0.5. From Figure 21, for a five pad load on pivot bearing, for the top unloaded pads

$$\phi_1 = 54°, \quad \phi_2 = 126°$$

From Equation (14)

$$m = \frac{0.5\sin 54°}{1+0.5\sin 54°}$$

$$m = 0.29$$

Thus, the top pads would become unloaded for preload values *less than* m = 0.29.

Example 2: Calculate the eccentricity ratio at which the top pads of a four pad, load between pivot bearing become unloaded. Assume that the tilting pad preload is m = 0.3.
For a four pad load between pivot bearing, for the top unloaded pads

$$\phi_1 = 45°, \quad \phi_2 = 135°$$

From Equation (15)

$$\varepsilon = \frac{.3}{1-0.3\sin 45°}$$

$$\varepsilon = 0.61$$

Thus, the top pads would become unloaded for bearing eccentricity values *greater than* ε = 0.61.

TILT PAD STATIC SHAFT SINK AND CLEARANCE MEASUREMENT

For between pivot loading, the journal can sink between the pivots, due to pad tilt. The amount of static shaft sink below the bearing center, S_s, is given in (Figure 22)

$$S_s = \frac{c'_b}{\cos\theta_p} \tag{16}$$

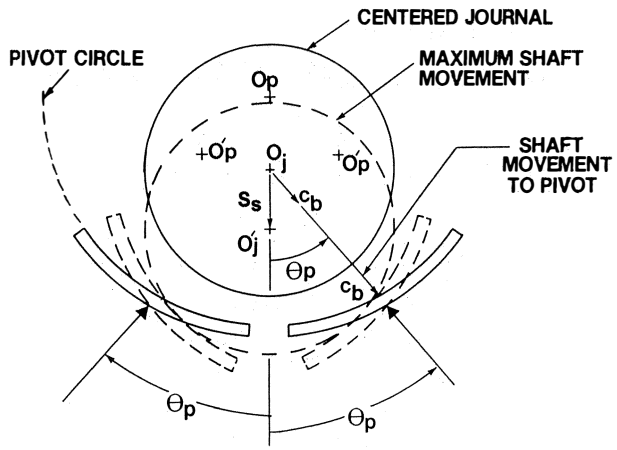

Figure 22. Tilting Pad Bearing Static Shaft Sink.

One method of measuring clearances for tilting pad bearings is to use a mandrel with a dial indicator. After the bearing is assembled around the mandrel, the bearing is pushed up against one of the pads directly toward the pivot. The dial indicator is zeroed and the bearing moved to between the opposite two pads. The dial indicator reading will be larger than the actual bearing clearance due to static shaft sink. This method of clearance measurement is employed for tilting pad bearings with an odd number of pads. For a four pad bearing, the clearance can be

measured from pad pivot to pad pivot directly without going between pads.

From Figure 23,

x = measured diametral clearance, in

n = # of pads

$$\theta_p = \frac{360°}{2 \cdot n}$$

$$X = c'_b + S_s$$

$$X = c'_b \left(1 + \frac{1}{\cos\theta_p} \right) \quad (17)$$

For a 5 pad bearing, $\theta_p = 36°$

$$X = c'_b (2.236)$$

$$X = \frac{c_b}{2} (2.236)$$

$$c_b = (0.894)X \quad (18)$$

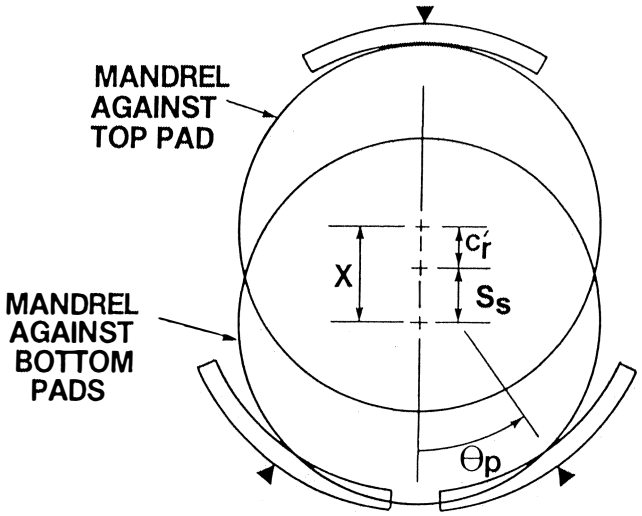

Figure 23. Tilting Pad Bearing Clearance Measurement.

NORMAL FORCE AND BREAKAWAY TORQUE

Two important parameters for bearing designers are normal force and breakaway torque. Normal force is the amount of the journal load that the babbitt actually experiences. This is important for bearings with high unit loads and/or high operating oil temperatures.

Breakaway torque, T, is the amount of torque necessary to turn the rotor after a prolonged down time. This calculation must be made to size turning gear motors. Define the following parameters

W_t = total rotor weight, lbf

$W = \frac{W_t}{2} \cong W_j$, journal load, lbf

For a plain journal bearing or an axial groove bearing

$$N_{ag} = W \quad \text{per bearing} \quad (19)$$

$$T_{ag} = \frac{D}{2} (\eta W) \quad \text{per bearing} \quad (20)$$

$$T_{ag} = \frac{D}{2} (\eta W_t) \quad \text{per rotor} \quad (21)$$

The above equations may also be used for a load on pivot tilting pad bearing. However, for load between pads, the bearing load is shared by the bottom 2 pads (Figure 22).

Thus,

$$N_{tp} = \frac{W}{2\cos\theta_p} \quad \text{per pivot} \quad (22)$$

From Equation (19),

$$N_{tp} = \frac{N_{ag}}{2\cos\theta_p} \quad (23)$$

For 4 and 5 pad load between pivot bearings:

$$\theta_p = 36°, N_{tp} = (0.62) \cdot N_{ag} \quad \text{5 pad between} \quad (24)$$

$$\theta_p = 45°, N_{tp} = (0.71) \cdot N_{ag} \quad \text{4 pad between} \quad (25)$$

Thus, there is

- 38 percent less babbitt load, five pad between
- 29 percent less babbitt load, four pad between

compared to sleeve bearings. Clearly, for bearings with high unit loads, a five pad load between pivot bearing would provide lower babbitt loads compared to sleeve bearings or load on pivot tilt pad bearings. Reducing babbitt load will decrease the tendency of a bearing to wipe at high loads and high babbitt temperatures.

These babbitt loads are nearly exact for startup calculations for all bearings. They are also fairly exact for plain journal, axial groove, and zero preloaded tilting pad bearings at operating speeds. The problem arises for sleeve bearings like the pressure dam or elliptical designs since, at operating speeds, the upper half produces additional hydrodynamic loads on the bottom loaded pad, thereby increasing the actual perceived babbitt load. The same scenario holds for preloaded tilting pad bearings.

From Equation (22), for a tilting pad bearing with load between pads,

$$N_{tp} = \frac{W}{\cos\theta_p} \quad \text{per bearing} \quad (26)$$

$$N_{tp} = \frac{W_t}{\cos\theta_p} \quad \text{per rotor} \quad (27)$$

and the break-away torque is

$$T_{tp} = \frac{\eta D W_t}{2\cos\theta_p} \quad \text{per rotor} \quad (28)$$

Comparing Equation (21) to Equation (28) yields

$$T_{tp} = \frac{T_{ag}}{\cos\theta_p} \quad \text{per rotor} \quad (29)$$

For 4 and 5 pad load between pivot bearings:

$$\theta_p = 36°, T_{tp} = (1.24) \cdot T_{ag} \quad \text{5 pad between} \quad (30)$$

$\theta_p = 45°$, $T_{tp} = (1.41) \cdot T_{ag}$ 4 pad between (31)

Thus, there is

- 24 percent more break away torque, five pad between
- 41 percent more break away torque, four pad between

compared to sleeve bearings. Thus, tilt pad bearings may require larger turning gear motors.

Example 3: One 250 lbf man can breakaway an axial compressor with a 10 f bar, when the rotor ran on axial groove bearings. Why cannot the same man breakaway the rotor with a 10 f bar after a bearing retrofit to four pad tilting pad bearings with load between pivots?

- W_t = 16,000 lbf
- D = 8.0 in
- c'_b = 6.0 mils
- c'_s = 5.0 mils

First, check the static shaft sink for the four pad bearing to ensure that the journal is not riding on the end seals. For a four pad bearing, θ_p = 45 degrees, and from Equation (16)

$$S_s = \frac{6.0}{\cos 45°}$$

$$S_s = 8.5 \text{ mils}$$

Recall that S_s is the static journal sink below the journals centered position. The amount that the journal sinks below the pivot circle is

$S'_s = S_s - c'_b$

$S'_s = 2.5$ mils

But, since $S'_s < c'_s$, the journal does not ride on the end seals.

Now calculate the breakaway torque.

Coefficient of friction:

- η = 0.2 steel on babbitt with thin oil film
- η = 0.44 steel on dry babbitt

Babbitt load (Equations (19) and (22)):

N_{ag} = 8,000 lbf/bearing

N_{tp} = 5,657 lbf/pivot

Breakaway torque for η = 0.44 (Equations (21) and (28)):

T_{ag} = 2,347 f-lbf

T_{tp} = 3,319 f-lbf

Thus, with a 10 f bar, the force necessary to breakaway the rotor is:

F_{ag} = 235 lb

F_{tp} = 332 lb

TILTING PAD BEARING OIL FLOW

One type of flow configuration used with tilting pad bearings is illustrated in Figure 24. The oil is distributed around the bearing by a circumferential inlet groove at the housing outside diameter. The inlet orifices direct the oil between each pad. Some oil is then discharged through the end seals. The majority of the oil leaves the bearing through large discharge holes at the top of the bearing housing.

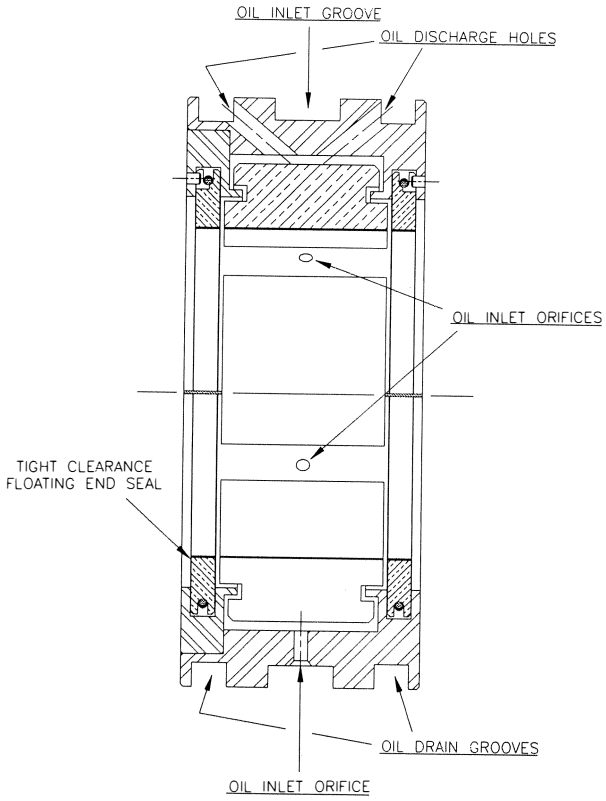

Figure 24. Non-Pressurized Housing Tilt Pad Bearing Design.

This flow configuration results in a nonpressurized housing with the flow restricted at inlet. The advantage of this setup is that most of the oil drains through the top of the bearing, into the twin circumferential drain grooves and directly into the drain cavity. Very little oil leaks through the relatively tight clearance floating end seals, keeping oil leaks to a minimum. The disadvantage is that hot oil produced by the lower loaded pads cannot exit directly, but must travel up through the bearing to the discharge holes.

The most common type of flow configuration used with tilting pad bearings is illustrated in Figure 25. All of the oil is discharged through end seals with relatively open clearances which can be fixed or floating.

This flow configuration results in a pressurized housing with the flow restricted at discharge. The advantage of this setup is that the hot oil produced by the lower loaded pads can exit directly through the end seal clearance. The disadvantage is that all the oil exits along the shaft making oil slingers and oil baffles necessary to prevent oil leaks.

A flow configuration that combines the advantages discussed above for Figures 24 and 25 is shown in Figure 26. Now, relatively tight end seals restrict the drain flow through the end seals minimizing oil leaks. The majority of the flow leaves the bearing through twin discharge holes between each set of pads. Thus, most of the oil drains directly into the drain cavity.

Flow calculations for tilting pad bearings are relatively simple since the flow is essentially speed and eccentricity independent. The flow depends only on inlet orifices, discharge orifices, end seal clearances and, to a lesser extent, oil viscosity.

The flows through the weep holes and oil inlet holes may be calculated from the orifice equation. The flow of an incompressible fluid through an orifice [5, p.3-62], is

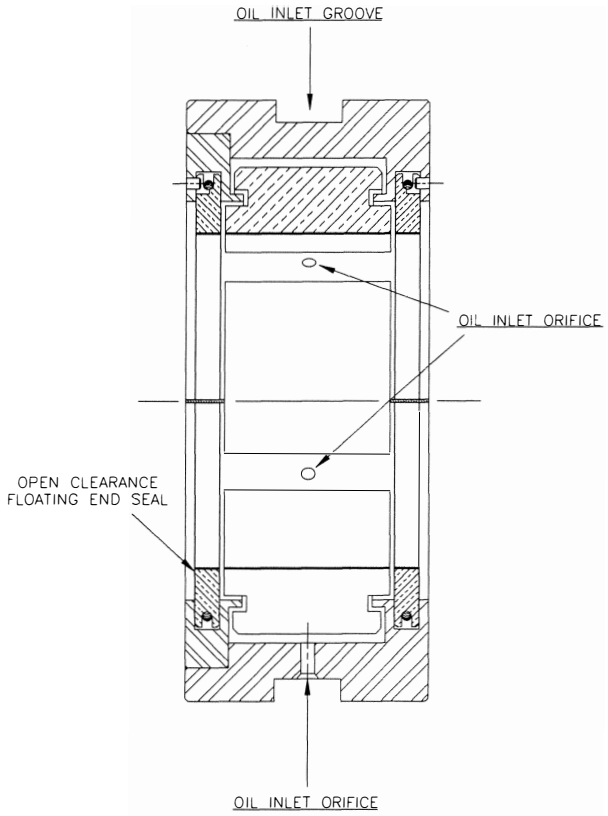

Figure 25. Pressurized Housing Tilt Pad Bearing Design.

$$Q = c_{cA}\sqrt{\frac{2\Delta P}{\rho}}$$

Assuming the following typical values for the density of oil and the flow coefficient through a short tube [5], page 3-70):

$$c_c = 0.61$$

$$\rho = 8.0 \times 10^{-5}\ \text{lbf} \cdot \text{s}^2 / \text{in}^4$$

$$Q = 25A\sqrt{\Delta P}\ \text{gpm} \qquad (32)$$

For n circular holes of diameter d

$$A = \frac{n\pi d^2}{4} \qquad (33)$$

$$Q = (19.64) \cdot nd^2\sqrt{\Delta P}\ \text{gpm} \qquad (34)$$

For the nonpressurized housing configuration of Figure 24 where the flow is restricted on inlet, the housing pressure, P_h = 0.0 and

$$\Delta P = P_{in} - P_h = P_{in}$$

$$Q = Q_{in} = (19.64) \cdot n_{in}d_{in}^2\sqrt{P_{in}}\ \text{(gpm)} \qquad (35)$$

Example 4. Calculate the oil flow for the tilting pad bearing of Figure 24 (nonpressurized housing) with the following flow configuration.

d_{in} = 0.1875 in

n_{in} = 5

P_{in} = 20 psig

P_h = 0.0 psig

From Equation (35) with $Q = Q_{in}$

$$Q = (19.64)(5)(0.1875)^2\sqrt{20}$$

$$Q = 15.4\ \text{gpm}$$

For the pressurized housing configuration of Figures 25 and 26 where the flow is restricted on discharge, the inlet flow from Equation (34) becomes

$$\Delta P = P_{in} - P_h$$

$$Q_{in} = (19.64) \cdot n_{in}d_{in}^2\sqrt{P_{in} - P_h}\ \text{(gpm)} \qquad (36)$$

Again, from equation (34), the oil flow through the discharge holes is

$$Q_o = (19.64) \cdot n_o d_o^2\sqrt{P_h - P_d}\ \text{(gpm)}$$

With the drain pressure, P_d = 0.0 pisg,

$$Q_o = (19.64) \cdot n_o d_o^2\sqrt{P_h}\ \text{(gpm)} \qquad (37)$$

The oil out the end seals may be approximated from equation (32).

$$Q_s = (25)A_s\sqrt{\Delta P_s}\ \text{(gpm)} \qquad (38)$$

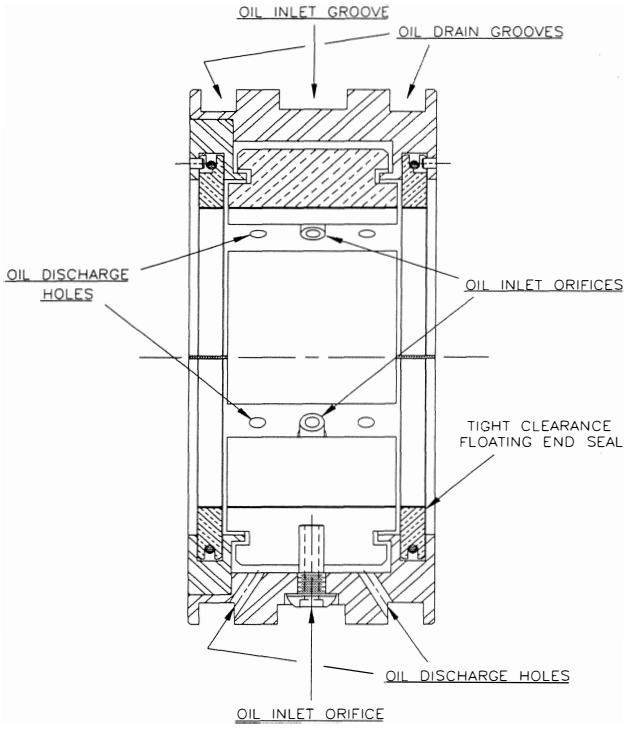

Figure 26. Pressurized Housing Tilt Pad Bearing Design with Oil Inlet Nozzles.

$$\Delta P_s = P_h - P_d = P_h \tag{39}$$

$$A_s = \frac{\pi n_s}{4}\left[(D + c_s)^2 - D^2\right] \tag{40}$$

Substituting (39) and (40) into (38) yields

$$Q_s = (19.64) \cdot n_s \left[(D + c_s)^2 - D^2\right] \sqrt{P_h} \quad \text{(gpm)} \tag{41}$$

Thus, the total bearing oil flow, Q, is equal to the inlet flow, Qin , which must be equal to the total drain flow, Q_d. The drain flow is the sum of the flow out of the end seals, Q_s , plus the flow out the discharge holes, Q_o.

$$Q = Q_{in} = Q_d = Q_s + Q_o \tag{42}$$

The steps necessary to size the inlet holes and calculate the oil flow for a tilt pad bearing with a pressurized housing are summarized below:

- For a given end seal clearance and discharge hole size, pick a housing pressure.
- From Equations (37), (41), and (42), calculate the drain flow, Q_d.
- From Equation (36), size d_{in} for $Q_{in} = Q_d$

Example 5. Size the oil inlet holes for a tilting pad bearing with the pressurized housing design of Figure 26. The following parameters are specified.

D = 4.0 in

c_s = 0.008 in diametral

d_o = 0.125 in

n_{in} = 5

n_o = 10

n_s = 2

P_{in} = 20 psig

First, pick a housing pressure. Typically, P_h = 5.0 psig

From Equations (37), (41), and (42), calculate the drain flow, Q_d.

From Equation (37), the flow out the discharge holes is

$$Q_o = (19.64)(10)(0.125)^2\sqrt{5}$$

$$Q_o = 6.9 \text{ gpm}$$

From equation (41), the flow out the end seal clearances is

$$Q_s = (19.64)(2)\left|(4.0 + 0.008)^2 - (4.0)^2\right|\sqrt{5}$$

$$Q_s = 5.6 \text{ gpm}$$

From equation (42), the total drain flow is

$$Q_d = 6.9 + 5.6 = 12.5 \text{ gpm}$$

From equation (36), size d_{in} for $Q_{in} = Q_d$

$$d_{in} = \left\{\frac{Q_{in}}{(19.64) \cdot n_{in}\sqrt{P_{in} - P_h}}\right\}^{1/2}$$

$$d_{in} = \left\{\frac{12.5}{(19.64)(5)\sqrt{(20 - 5)}}\right\}^{1/2}$$

$$d_{in} = 0.18 \text{ in}$$

TEMPERATURE RISE

The bearing temperature rise, ΔT, is defined as the difference between the inlet temperature and the drain temperature.

$$\Delta T = T_d - T_{in} \ ^\circ F \tag{43}$$

From Equation (7-34) [6, page 204],

$$T_d = T_{in} + \frac{42.2(HP - \Phi)}{\hat{c}_p Q} \ ^\circ F$$

For bearings larger than D = 2.0 in, the heat loss due to conduction and radiation may be neglected [6]. With a typical value for oil of $\hat{c}_p$ = 3.5 (density = 7.0 slug/gal, specific heat = 0.5 BTU/(slug × °F) for light turbine oil (ISO 32) at about 170°F),

$$\Delta T = 12.0\left(\frac{HP}{Q}\right) \ ^\circ F \tag{44}$$

From Equation (44), as the flow increases, the temperature decreases as expected. Also, as ΔT and/or Q increase, the power loss increases. An ideal bearing design provides just enough oil flow to cool the bearing to just below the acceptable maximum babbitt temperature. Any additional oil would lower this maximum temperature, but would increase the power loss.

Usually, bearings are designed with a maximum temperature margin. That is, the flow is increased slightly above the required minimum so that the bearing operates at a temperature that is slightly below the maximum.

REDUCED TEMPERATURE TILTING PAD DESIGNS

With speeds and/or loads increasing, bearings often operate near or above the maximum babbitt temperature limit. Increasing the oil flow to further cool the bearing produces exponential results. That is, a 10 percent increase in flow may produce a 10 percent decrease in temperature whereas a 20 percent flow increase would only result in a 12 percent temperature decrease.

Another approach is to make the cool inlet oil more effective in cooling the bearing. For tilting pad bearings, a substantial percentage of the hot oil is carried over by the shaft from the trailing edge of one pad into the leading edge of the next pad (Figure 27). This carryover is of the order of 50 to 60 percent. One way to more effectively cool the bearing is to reduce this carryover. The less the carryover, the cooler the oil is as it enters the leading edge of each pad.

One method of reducing the carryover is to introduce cool inlet oil directly into the pad leading edge as shown in Figure 28 [7]. This effectively blocks some of the hot oil carryover while it introduces more cooling oil into the pad.

Another method is the spray bar illustrated in Figure 29. Here, oil is distributed across the axial length of the pad by the spray bar. Again, this oil spray blocks some of the hot oil carryover and increases the flow of cool inlet oil into the pads.

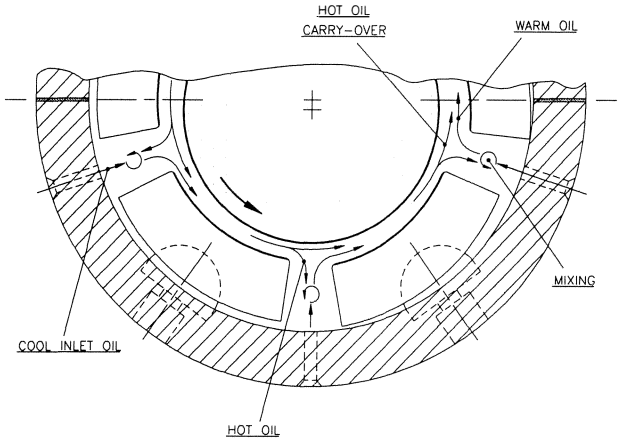

Figure 27. Pad-to-Pad Hot Oil Carryover.

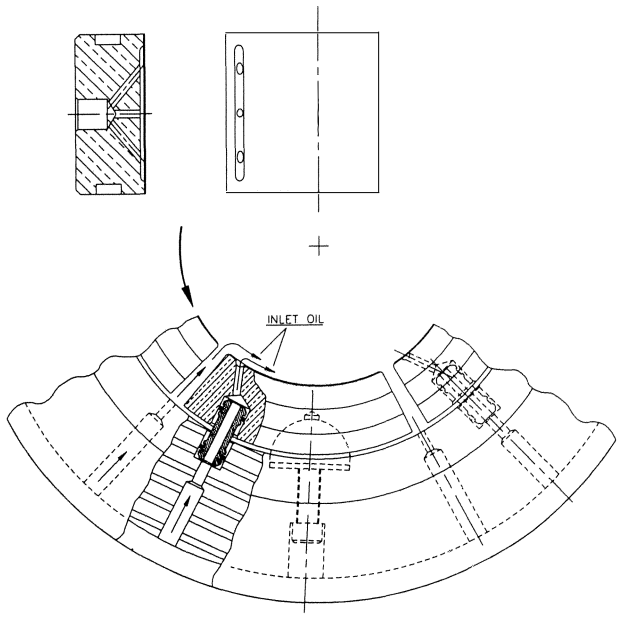

Figure 28. Leading Edge Feed Groove Tilt Pad Bearing Design.

An additional feature of this design is the open inner end seals that allow the oil to exit the bearing directly. Additional discharge holes are located in pairs between each set of pads. This discharge configuration allows the bearing to run in a completely evacuated housing which further reduces the bearing temperature by eliminating entrapped hot oil [8].

Any of these directed lube features can be successful in lowering the bearings maximum operating temperature for bearings that are running hot. A conservative rule of thumb is about a 10 percent temperature decrease. For bearings that are not running hot, the oil flow may be decreased which results in a power loss savings.

One disadvantage of an evacuated cavity (Figure 29) is that the bearings would not be able to operate as long as a conventional bearing (Figures 24, 25, and 26), if there is a sudden loss of the oil supply. However, directed lube, evacuated cavity thrust bearing designs have been in service for many years without apparent problems associated with sudden oil supply loss.

Test results for two steam turbine tilt pad bearings are shown in Figures 30, 31, 32, and 33 comparing pad embedded thermo-

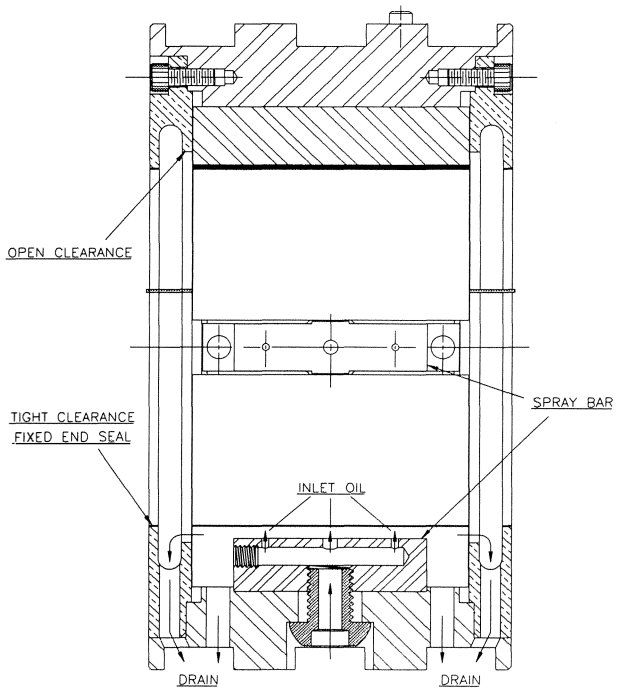

Figure 29. Evacuated Housing Spray Bar Tilt Pad Bearing Design.

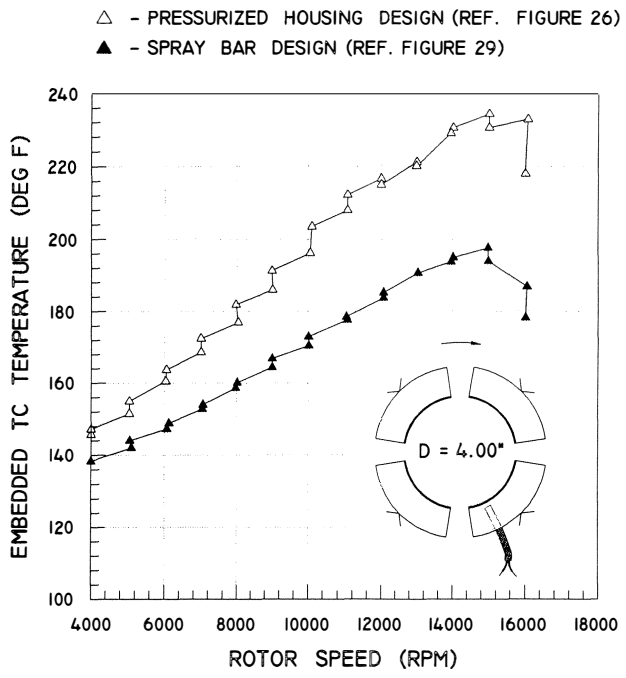

Figure 30. Spray Bar Vs *Pressurized Housing Metal Temperature Comparison—Upstream Pad, Exhaust End.*

couple temperature readings (*vs* speed) for the pressurized housing design of Figure 26 to the spray bar design of Figure 29. Exhaust end bearing data is shown in Figures 30 and 31, while results for the steam end bearing are presented in Figures 32 and 33. Note that the reduced pad temperatures for the spray bar designs are of the order of 10 percent. Specifically, from Figure

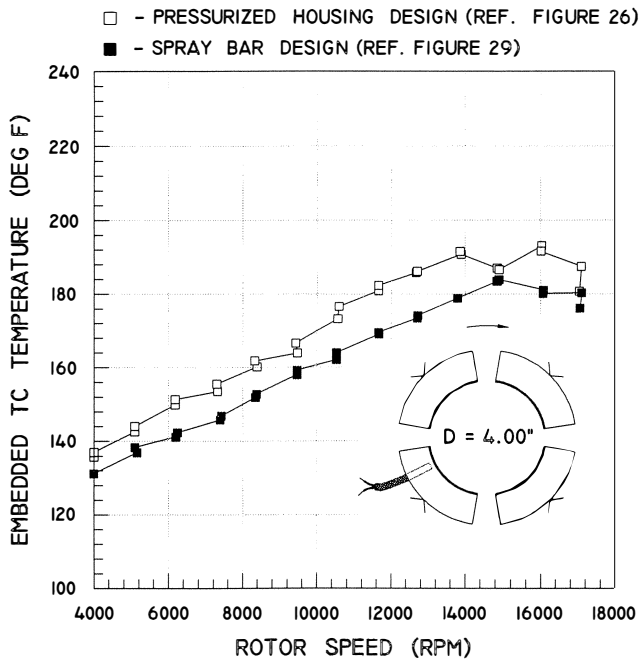

Figure 31. Spray Bar Vs *Pressurized Housing Metal Temperature Comparison—Downstream Pad, Exhaust End.*

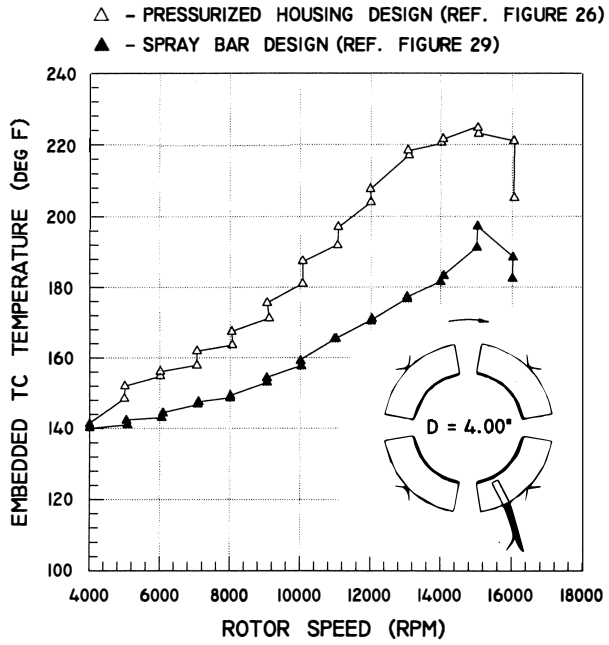

Figure 32. Spray Bar Vs *Pressurized Housing Metal Temperature Comparison—Upstream Pad, Steam End.*

30 (the exhaust end upstream pad), the maximum TC reading is about 235°F for the pressurized design compared to about 200°F for the spray bar design. Similar results are evident in Figures 31, 32, and 33.

CONCLUSIONS

The major conclusions concerning tilting pad bearing design are summarized below. These conclusions and recommendations are meant to be general *guidelines* and may not hold for all rotor-bearing systems.

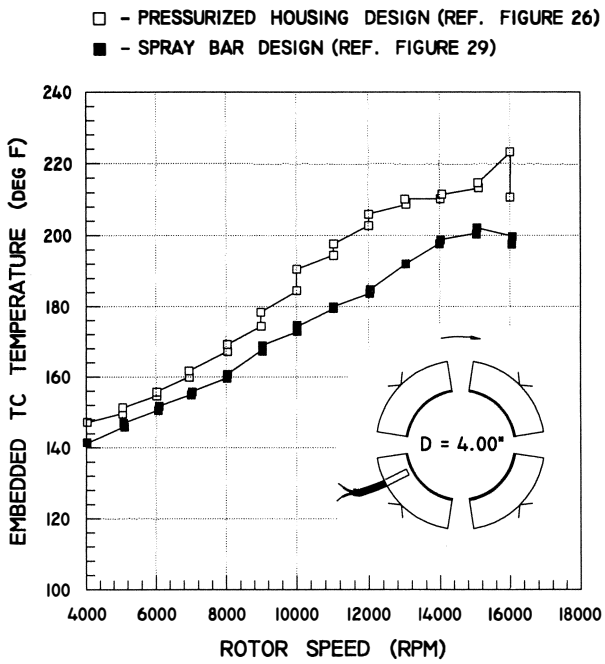

Figure 33. Spray Bar Vs *Pressurized Housing Metal Temperature Comparison—Downstream Pad, Steam End.*

Recommended limits of operation.

- Bearing unit loading: $L_u \leq 200$ psi
- Journal surface speed: $U_s \leq 300$ f/s
- Maximum metal temperature:
  - $T_{max} \leq 185$°F design (analytical prediction)
  - $T_{max} \leq 200$°F test acceptance
  - $T_{max} \geq 230$°F alarm
  - $T_{max} \geq 250$°F trip

Geometric properties.

- Pad pivot offset.
  - Load capacity increases as offset increases.
- Pad preload.
  - As preload decreases, effective damping increases thereby increasing forced response attenuation and improving stability.
  - As preload decreases, the top pads become unloaded, bearing damping decreases and the unloaded pads flutter.
  - Negative preload should be avoided as horizontal stiffness and damping decrease drastically as the preload becomes negative.
- Pad length-to-diameter ratio.
  - As L/D increases, the bearing effective damping increases, thereby increasing forced response attenuation and improving stability.

Clearance measurement.

- For a five pad tilt pad bearing, measuring the journal movement from the center of one pad to between the adjacent

two pads results in overestimating the bearing clearance by about 10 percent.

Babbitt load.

- Compared to sleeve bearings, there is 38 percent less babbitt load for a five pad load between pivot bearing.
- Compared to sleeve bearings, there is 29 percent less babbitt load for a four pad load between pivot bearing.

Break away torque.

- Compared to sleeve bearings, there is 24 percent more break away torque for a five pad load between pivot bearing.
- Compared to sleeve bearings, there is 41 percent more break away torque for a four pad load between pivot bearing.

Reduced temperature designs.

- Test results show about a 10 percent maximum metal temperature reduction for a spray bar design with an evacuated cavity, compared to a conventional pressurized housing design.

NOMENCLATURE

A	area (in^2)
A_s	end seal area (in^2)
c, c'	bearing diametral, radial clearance (in)
c_b, c'_b	tilt pad bearing diametral, radial clearance (in)
c_p, c'_p	pad diametral, radial clearance (in)
c_s, c'_s	end seal diametral, radial clearance (in)
$\hat{c}_p$	specific heat (BTU/(gal-°F))
c_c	flow coefficient (dim)
C	bearing damping (lbf-s/in)
$\overline{C}$	dimensionless bearing damping (dim)
C_{xx}, C_{yy}	bearing damping in the horizontal, vertical direction (lbf-s/in)
$\overline{C}_{xx}, \overline{C}_{yy}$	dimensionless bearing damping in the horizontal, vertical direction (dim)
D	journal diameter (in)
d	diameter (in)
d_{in}, d_o	oil inlet, discharge orifice diameter (in)
e	bearing eccentricity (in)
F_x, F_y	horizontal, vertical forces (lbf)
F_{ag}, F_{tp}	axial groove, tilt pad bearing forces (lbf)
h_p	pivot film thickness (in)
$\overline{hp}$	dimensionless pivot film thickness (dim)
HP	power loss (hp)
K	bearing stiffness (lbf-s/in)
$\overline{K}$	dimensionless bearing stiffness (dim)
K_{xx}, K_{yy}	bearing stiffness in the horizontal, vertical direction (lbf/in)
$\overline{K}_{xx}, \overline{K}_{yy}$	dimensionless bearing stiffness in the horizontal, vertical direction (dim)
L	bearing axial length (in)
L_u	bearing unit load (psi)
m	tilt pad bearing preload (dim)
N, N_s	journal rotational speed (rpm, rps)
n	number of tilting pads (dim)
n_s, n_o, n_{in}	number of oil seals, outlet or discharge holes, inlet orifices (dim)
N_{ag}, N_{tp}	axial groove, tilt pad bearing normal force (lbf)
O_b, O_p, O_j	bearing, pad, journal center (dim)
P	pressure (psig)
ΔP	pressure drop (psig)
ΔP_s	pressure drop across the end seal (psig)
P_{in}, P_h, P_d	inlet, housing, drain pressure (psig)
Q	oil flow (gpm)
Q_{in}, Q_d	inlet, drain oil flow (gpm)
Q_s, Q_o	oil flow out the end seals, discharge holes (gpm)
R	journal radius (in)
R_b, R_p	bearing radius, pad radius of curvature (in)
S	Sommerfeld number (dim)
S_s	static shaft sink below centered position (in)
S'_s	static shaft sink below pivot circle (in)
ΔT	temperature rise (°F)
T_{in}, T_d, T_{max}	inlet, drain, maximum temperature (°F)
T_{ag}, T_{tp}	axial groove, tilt pad bearing break away torque (f-lbf)
U_s	journal surface velocity (f/s)
W_t	total rotor weight (lbf)
W_j	journal load (lbf)
$W = W_t/2$	approximate journal load (lbf)
X	measured diametral clearance (in)
X,Y	horizontal, vertical coordinates (dim)
α	tilt pad pivot offset (dim)
ε	bearing eccentricity ratio (dim)
η	coefficient of friction (dim)
θ, θ'	circumferential bearing coordinates (dim)
θ_p	angle to tilt pad pivot from bottom dead center (deg)
μ	oil viscosity (lbf-s/in^2)
ρ	oil density (lbf-s^2/in^4)
Φ	heat loss due to conduction and radiation
ϕ_p	angle from tilt pad leading edge to pivot (deg)
ϕ_1, ϕ_2	angle to first, second tilt pad pivot from +x axis (deg)
Ψ	bearing attitude angle (deg)
ω	journal rotational speed (1/s)

REFERENCES

1. Nicholas, J. C., Gunter, E. J., and Allaire, P. E., "Stiffness and Damping Coefficients for the Five Pad Tilting Pad Bearing," ASLE Transactions, *22* (2), pp. 112-124 (April 1979).
2. Nicholas, J. C., Gunter, E. J., and Barrett, L. E., "The Influence of Tilting Pad Bearing Characteristics on the Stability of High Speed Rotor-Bearing Systems," *Topics in Fluid Film Bearing and Rotor Bearing System Design and Optimization*, an ASME publication (April 1978).
3. Nicholas, J. C. and Kirk R. G., "Four Pad Tilting Pad Bearing Design and Application for Multi-Stage Axial Compressors," ASME Journal of Lubrication Technology, *104* (4), pp. 523-532 (October 1982).
4. Nicholas, J. C. and Kirk, R. G., "Selection and Design of Tilting Pad and Fixed Lobe Journal Bearings for Optimum Turborotordynamics," *Proceedings of the Eighth Turbomachinery Symposium*, The Turbomachinery Laboratory, Texas A&M University, College Station, Texas (1979).
5. *Marks Standard Handbook for Mechanical Engineers, Ninth Edition*, New York, New York: McGraw Hill (1987).

6. Wilcock, D. F., Booser, E. R., *Bearing Design and Application*, New York, New York: McGraw Hill (1957).

7. Dmochowski, W., Brockwell, K., DeCamillo, S., Mikula, A., "A Study of the Thermal Characteristics of the Leading Edge Groove and Conventional Tilting Pad Journal Bearings," ASME Journal of Tribology, *115*, pp. 219-226 (April 1993).

8. Tanaka, M., "Thermohydrodynamic Performance of a Tilting Pad Journal Bearing with Spot Lubrication," ASME Journal of Tribology, *113*, pp. 615-619 (July 1991).